Functional characterization of Lipid storage droplets 1 (LSD1) in growth and lipolysis of *Hermetia illucens*

Yuguo Jiang[ab], Zongqing Kou[ab], Bihui Chen[ab], Xingyu, Luo[ab], Yongping Huang[a]

[a] CAS Key Laboratory of Insect Developmental and Evolutionary Biology, CAS Center for Excellence in Molecular Plant Sciences, Institute of Plant Physiology and Ecology, Chinese Academy of Sciences, Shanghai, China

[b] University of Chinese Academy of Sciences, Beijing, China

Keywords: *Hermetia illucens*, perilipin, lipid homeostasis, CRISPR/Cas9, growth, fatty acid

Abstract

As intracellular organelles in adipose tissue, lipids droplets manage the balance between triglyceride accumulation and energy consumption in animals. Perilipin family members, associated with surface of lipid droplets, participate the regulation of lipid metabolism. Lipid storage droplet-1 (LSD1)/Perilipin-1 acts as a gatekeeper for adipose lipid storage in animals. Despite extensive studies in fruit fly, the function of *LSD1* in insect larval stage remain indistinct. In this study, we characterized the function of *LSD1* in black soldier fly *Hermetia illucens*, a nova resource insect to recycle organic wastes. We found that *LSD1* was broadly present in dipteran species and evolved with divergence between mosquitos and flies. We further constructed *in vivo* mutagenesis mediated by CRISPR/Cas9 and found that mutations in *LSD1* increased the larval weight and did not bring any defects in development. Raw fat content was also not significantly influenced in late larval stage and new-emerged adults. Our results not only extend our knowledge of *LSD1* in insects, but also help for better understanding of the lipid homeostasis in BSF.

Introduction

Lipid homeostasis, balance between lipogenesis, storage, and lipolysis, is fundamental for growth, development, and reproduction in living organisms. In insects, fat body, primarily composed of adipocytes, is the hub of lipid storage and metabolism (Li et al., 2019). As the core intracellular organelle in adipocytes, lipid droplets (LDs) play

the critical role in lipid homeostasis. LDs consist of a monolayer of phospholipid with a triglyceride (TAG) core, which is proposed to be formed from endoplasmic reticulum (Walther et al., 2017). For lipogenesis, fatty acids, hydrolyzed form diet lipids or synthesized *de novo*, serve as acyl donors for the esterification. TAG, as the terminal product, will be transported into LDs for storage. To responded to the energy demand, TAG will be disintegrated back into glycerol and fatty acids by lipid lipases located on the surfaces of LDs and the fatty acids will go through continuous beta-oxidation to produce energy (Arrese & Soulages, 2010).

The accumulation of triglycerides in fat body tissues is a balanced results of the dynamics between neutral lipogenesis and lipolysis. For lipolysis, perilipins is the key factor to recruit lipases from cytoplasm to LDs (Brasaemle, 2007). In *Drosophila melanogaster*, two perilipins family members are encoded, *Lipid storge droplet-1(LSD1)/ Perilipin-1* and *LSD2/Perilipin-2* (Lu et al., 2001). *DmLSD1* is expressed during all ontogenesis stages (Beller et al., 2010) and the protein is exclusively located on the surface of LDs in larval fat body (Bi et al., 2012). Opposite the guardian function of DmLSD2 to obstruct lipolysis, DmLSD1 could stimulate lipolysis through adipokinetic hormone (AKH) signaling pathway or by recruitment of lipases to LDs surface(Kimmel & Sztalryd, 2016). In fruit fly, absence of *LSD1* suppressed both above mentioned mechanisms and increased adiposity in adults (Bi et al., 2012). In fruit fly, a few study mentioned the changes in glyceride accumulation in larval stage of *lsd1*. Although under fed condition, average area of single LD was significantly increased in *lsd1* larvae compared with wild type, the total glyceride was not changed in *lsd1* mutants except that under starvation condition (Bi et al., 2012). In other non-drosophila insects, the species-specific functions of perilipins in lipid accumulation or lipolysis have not been demonstrated.

The black soldier fly (BSF), *Hermetia illucens* (L.) (Diptera: Stratiomyidae) has attracted extensive attention as one of the most promising insects that are qualified in organic wastes recycling (Raksasat et al., 2020; Surendra et al., 2020; Kim et al., 2021). This species could efficiently assimilate various organic substrates into biomass composed of protein, fat, and chitin, which are valuable raw materials or ingredients for industries and animal husbandry (Huis et al., 2020; Hawkey et al.,

2021; Niyonsaba et al., 2021). Great potentials are held in BSF for its nutritional value. For the inside grease, after extraction, separation, and refinement, could be added into feed (Fawole et al., 2021; Heuel et al., 2021) or cosmetic products (Almeida et al., 2020) as gradients, depending on the depth of refinement, or as raw materials for biodiesel (Zheng et al., 2012; Nguyen et al., 2017; Wang et al., 2017) and biolubricants (Xiong et al., 2020) after transesterification. BSF, as a nova resource insect, is worthy of conducting research on functions of perilipins in lipid homeostasis to maximize its advantages for application.

In our study, *HiLSD1* was cloned from genome of *H. illucens* and two homozygote mutants of *HiLSD1* were obtained based on CRISPR/Cas9 platform. The function role of *HiLSD1* in larval development was initially characterized by growth assay. Besides the influences on lipid droplets forming, we also investigated whether and how *Hilsd1* change the fat accumulation and fatty acids profiles. The results will not only extend our knowledge of *LSD1*, but also help for better understanding of lipid metabolism in BSF.

Materials and Methods

1. Rearing of BSF strains

The laboratory-maintained wild-type line of BSF, which was originally collected from Dr. Ziniu Yu's lab, underwent inbred crossing for generations in our lab (Zhan et al., 2019). The newly hatched larvae, wild type, or mutants were reared in moistened wheat bran (1:2 ratio of dry matter/ddH_2O) under an 8:16 L:D photoperiod at 28°C with relative humidity of 50%-60%.

2. Clone of *LSD1* in BSF

The amino acid sequence of LSD1 in *D. melanogaster* (NP_001262883.1) was used as a query to search the ortholog in the genome of the BSF (GCF_905115235). Based on manual annotations, the architecture of ORF were predicted. Polymerase chain reaction (PCR)-amplification was applied to obtain coding sequence from complementary DNA (cDNA) with the following pair of primers: forward, 5'-ATGGTTAAGCAACAGATAAAACG-3' and reverse, 5'-TCAATAAACTCCATTTAAATTGTTC-3'. For cDNA synthesis, total RNA was

100 isolated from 3rd larval instar of wild-type strain using TRIeasyTM Total RNA
101 Extraction Reagent (Yeasen, Shanghai, China). One μg of total RNA was processed
102 using PrimeScript RT reagent Kit with gDNA Eraser (Takara, Beijing, China). The
103 PCR procedure was set as follows: 98℃ for 2 min, followed by 30 cycles at 98℃ for
104 30 s, 55℃ for 30 s, 68℃ for 1 min, and an elongation phase at 68℃ for 10 min.
105 Amplified products were sequenced and verified after cloning into a pJET1.2-T
106 vector through CloneJET PCR Cloning Kit (Thermo Scientific, Waltham, USA).
107
108 3. Comparative and phylogenetic analysis of LSD1
109 The protein sequence of HiLSD1 was used as a query to search dipteran orthologs
110 against Genbank nonredundant protein database (nr) using BLASTP. The sequences
111 from 8 representative dipteran species were used for further analysis (*Aedes aegypti*,
112 XP_021693334.1; *Anopheles gambiae*, XP_312022.5; *Culex quinquefasciatus*,
113 XP_001845547.2; *Bactrocera dorsalis*, XP_011212558.1; *Ceratitis capitata*,
114 XP_004523385.1; *Drosophila melanogaster*, NP_001262883.1; *Lucilia cuprina*,
115 XP_023297473.1; *Musca domestica*, XP_005189534.1;) with a lepidopteran species
116 as reference (*Manduca sexta*, ACF24761.1). Protein sequences of HiLSD1 and
117 orthologous sequences were subjected to multiple alignment and phylogenetic
118 analysis using MEGA X (Li et al., 2022). The phylogenetic tree was inferred using
119 the maximum likelihood method with a bootstrap of 1000 replications. The tree was
120 rooted using the ortholog of *Manduca sexta* as the outgroup.
121
122 4. CRISPR/Cas9-mediated construction of *lsd1* homozygotes
123 For CRISPR/Cas9-mediated mutagenesis of *LSD1*, with the PAM sequences in
124 consideration, newly designed sgRNAs should follow the NNN19GG rule (Zhan et
125 al., 2019). Based on sequence identification of *HiLSD1*, four 23-bp sgRNA targeting
126 sites named S1-4 (Table S1) were designed by Geneious Prime 11.0.3. sgRNA
127 templates were transcribed using a T7 promoter and synthesized *in vitro* using the
128 MAXIscript T7 kit (Ambion, Austin, USA) according to the manufacture's
129 instruction. The Cas9 protein was purchased form Thermo Scientific.
130 Germline transformation was performed as described previously (Zhan et al., 2019).
131 Briefly, Cas9 protein (200 ng/μL) with two sgRNAs (100 ng/μL) were co-injected
132 into embryos. After hatching, first instar larvae were selected to detect genomic

133 mutations with primers listed in Table S2. The amplified fragments were cloned into
134 pJET1.2 for sequencing. Frame-shift mutants were reared in moistened wheat bran for
135 inbreed crossing to obtain homozygotes.
136
137 5. Growth assay of *lsd1*
138 To verify the effect of *lsd1* on larval growth, 4th day larvae, wild type and *lsd1*, were
139 reared in a chamber with temperature, relative humidity and fluorescent photoperiod
140 set to 28 °C, 60% RH and 8:16 (L:D). Sixty larvae of each genotype were placed into
141 individual plastic basin (500 mL) with three replicates. One hundred gram of
142 moistened wheat bran (1:2 ratio of dry matter/ddH_2O) were refreshed every 24 hours
143 until over 75% of larvae reached prepupal stage. Before routine reloading, weight of
144 all larvae in each basin was recorded, as well as the number of survived and
145 development stage at that very moment. The larval stage was determined by mouth
146 morphology characteristics (2015-Kim). The larvae collected at 7 days, 12 days and
147 22 days post hatching were defined as L4, L5 and prepupae, respectively. All
148 collected larvae for further chemical analysis were stored in -80°C after inactivation
149 by liquid nitrogen.
150
151 6. Feed experiment
152 The feeding trials, starting with 7th day larvae (around the middle of L4), were under
153 the same rearing condition as mentioned above. Sixty larvae were fed twice, being on
154 days 1 and 4, with 120 g moistened wheat bran. The initial weight was monitored by
155 weighing 20 larvae for each sample. At the end of trials on day 12, larvae were
156 separated from the remaining residues and weighed. The dry matter content of
157 residues and larvae was determined after dried in oven.
158
159 Bioconversion efficiency (BE), feed conversion ratio (FCR), waste reduction (WR)
160 and efficiency of conversion of digested feed (ECD) were calculated as previously
161 reported (Broeckx et al., 2021; Ribeiro et al., 2022):
162
163 $BE = (DW_{larvae,\ end} - DW_{larvae,\ start}) / DW_{feed} \times 100\%$
164 $FCR = DW_{feed} / (FW_{larvae,\ end} - FW_{larvae,\ start})$
165 $WR = (DW_{feed} - DW_{residue}) / DW_{feed} \times 100\%$

$ECD = (DW_{larvae, end} - DW_{larvae, start}) / (DW_{feed} - DW_{residue}) \times 100\%$

Where DW is the dry weight and FW is the fresh weight.

7. Lipid droplet staining and microscope

Fat body tissue from 11-day-old larvae (middle 5th instar stage) was prepared as follows for *ex vivo* confocal laser scanning microscopy. The body of 5th-instar larva was opened, and the fat body tissues attached to the cuticle mechanically released into mounting medium (50% glycerol/PBS, Nile red [Sigma, stock 10% in DMSO] 1:5000, Hoechst 33342 [Beyotime, stock in 10 mg/mL] 1:1000). The tissue was analyzed within 2h after mounting using a Leica Stellaris 5 with 405 nm excitation/420-471 nm emission wavelength range for Hoechst and 561 nm excitation/570-630 nm emission wavelength range for Nile red.

8. Quantification of raw fat content

All collected larvae or adults for chemical analysis were dried in an oven at 60°C for 72h and reweighed to determine water content. The total fat content of BSF was determined using the standard protocol (GB/T 5009.6-2016). Briefly, 1 g of the dried sample was ground and subjected to Soxhlet extraction with n-hexane(AR, Sinopharm) at 75°C overnight. After vacuum evaporation, the extracts were weighed to determine the raw fat content.

9. Analysis of fatty acid profiles

The fatty acid profiles of extracted raw fat were measured using the standard method (GB/T 5009.168-2016). Briefly, 50 mg sample was put into 5 mL glass vial with 1 mL of NaOH-MeOH solution (2%, w/v) for saponification. To obtain the methyl ester solution, 1mL BF_3-MeOH (14%, sigma) was added into the vial for 15 min, followed with 2 mL n-hexane to extract the products. Finally, the fatty acid methyl esters (FAMEs) were determined by gas chromatography.

An GC2010 pro (Shimazu, Suzhou, China) was equipped with a TG-WaxMS capillary column (60 m × 0.25 mm × 0.25 μm, Thermo scientific) and a flame ionization detector (FID). The GC program was as follows: initial temperature of 120 °C; ramp to 240°C at rate of 5°C/min, maintain 6min. The temperature of inlet and detection were 220°C and 240°C, respectively. The sample volume of per

199 injection was 2 μL in split ratio of 40. The flow rate of carrier gas (nitrogen) was kept
200 at 1.5 mL/min. Qualitative analysis was conducted by authentic compounds
201 purchased from Sigma. Fatty acid relative content was quantified by percentage of
202 weight of each fatty acid in raw fat, which was calculated by external standard
203 method.
204
205 10. Investigation of expression of relevant genes
206 Relative expression of several genes in insulin signaling pathway and lipid
207 homeostasis network from 11-day-old larvae (middle 5th instar larval stage) was
208 determined in *lsd1* mutant and WT. Total RNA was extracted from fat body of larvae
209 and subsequently reverse-transcribed into cDNA as mentioned above. The transcript
210 levels were assayed using SYBR Green Master Mix (TOYOBO) normalized against
211 *HiActin* (Gao et al., 2019). The primers are listed in Table S3.
212
213 11. Statistics
214 A two tail Student's t-test was used to analyze the differences between results unless
215 otherwise noted. Bar charts were drawn and analyzed with GraphPad PRISM 8.0
216 software (San Diego, California, USA). Three independent replicates were used for
217 each test. Error bars represent the standard deviation (S.D.).
218
219 **Results**
220 1. Characterization of *HiLSD1* in the genome
221 To identify sequence of *HiLSD1*, the protein sequence of *LSD1* in *D. melanogaster*
222 (NP_001262883.1) was used to characterize the ortholog (*HiLSD1*) in genome of
223 *Hermetia illucens* (GCF_905115235) (Generalovic et al., 2021). *HiLSD1* is located on
224 chromosome 1 and spans 14433-bp genomic sequence, which consists of 7 exons and
225 encodes a 398-amino acid protein (Fig. 1A). Using *HiLSD1* as a query for BLAST,
226 we found that most dipteran insect, especially representative flies, and mosquitos,
227 encoded *LSD1* in their genome, but nevertheless shares a relatively low amino acid
228 identity (from 54.50% in *Bactrocera dorsalis* to 57.18% in *Drosophila*
229 *melanogaster*). In addition, the phylogenetic analysis of dipteran *LSD1* orthologs
230 showed that the topology of the gene tree greatly agreed with that of the species tree
231 by previous study (2019-CR)(Fig. 1B), which implied that the evolution of *LSD1* may

232 correlate with the speciation across dipterans. To conclude, above results reveal that
233 LSD1 is broadly present in dipterans and under conserve evolution across species.
234
235 2. Mutagenesis of *Hillsd1* mediated by CRISPR/Cas9
236 To further investigate the function of HiLSD1 in BSF, an *in vivo* knock-out was
237 conducted mediated by CRISPR/Cas9 system (Fig. 2A). Two pairs of sgRNAs,
238 Target site 1/ Target site 2 (TS1/TS2) and Target site 3/ Target site 4 (TS3/TS4) were
239 designed in preceding exons following the NNN19GG rule (Fig. 2B). The
240 transformation was performed on fresh laid eggs with microinjection equipped with
241 200 ng/μL Cas9 protein and 100 ng/μL for each paired sgRNAs. Newborns of G1
242 were selected to detect the mutations. Positive mutants were reared generations for
243 inbreed crossing to obtain homozygotes (Fig. 2A). Both homozygotes shown in Fig.
244 2B were obtained in G3 offspring after mutation detection for over 10 egg clutches in
245 each generations. Both mutants showed disruption in amino acid sequences of
246 HiLSD1 and caused premature translational termination, indicative of at least partial
247 function loss. It should be noted that design of pair sgRNAs located in exons was for
248 large fragment deletion, which did not happen(Fig. 2B). Adjustment of Cas9 and
249 sgRNAs concentration, along with selection of sgRNAs for higher theoretical
250 efficiency, would increase the chance for large fragment deletions.
251
252 3. Improvement in larval growth by *Hilsd1*
253 To investigate the influence in growth by *Hilsd1*, a growth assay was conducted
254 among two mutants and wild type (WT). For incubation, similar size and average
255 weight was considered to control the initial larval conditions. Daily refreshed
256 moistened wheat bran as food is guaranteed to be sufficient. For larval weight during
257 the development, both *lsd1* mutants achieved significant heavier body than WT (Fig.
258 3A). For WT, maximum average weight, 0.2210 g, appeared at 269h (around 11 days
259 after hatching), which was late stage of 5th instar larvae. Then the average weight
260 decreased, and the larvae began to pre-pupate. Meanwhile, both *lsd1* mutants were
261 still in weight growth, 0.2416 g of *lsd1*(-6,-7) and 0.2320 g of *lsd1*(-2, -2), which were
262 9.30% and 4.98% heavier than WT, respectively. Maximum average weight of *lsd1*
263 reached at 295h, the time that prepupation had begun in all groups. The average
264 weight of *lsd1*(-6,-7) was 0.2504 g and that of *lsd1*(-2,-2) was 0.2400 g, which were

265 15.67% and 10.85% heavier than WT with little decreased weight (0.2165 g) at that
266 timepoint, respectively. After that, weight of larvae in all groups decreased caused by
267 prepupation and pupation. Both mutants maintained a significant advantage in weight
268 until 18 days after hatching (around 440h). At the end of pupae stage, when the first
269 eclosion appeared, rest of all pupae were weighed and pictured. For *lsd1*(-6,-7), mean
270 of pupae weight was significantly little heavier than WT (7.24%, WT: 0.1380 g;
271 *lsd1*(-6,-7): 0.1480 g) (Fig. 3B).
272 For development, the mutant would little early reach 50% prepupation (Fig. 3C) and
273 50% pupation (Fig. 3D), especially in a situation that first prepupae and pupae always
274 appeared in WT group. As illustrated, pupae of *lsd1*(-6,-7) were little larger than that
275 of WT. Taken together, disruption of *HiLSD1* did not bring any apparent defects in
276 larval growth and development, even improve the growth in larval stage instead.
277
278 4. The better feeding performance of *Hilsd1*
279 To further elucidate the reason of improved growth in *Hilsd1*, a feeding trial was
280 performed during L4-L5 (7 day – 12 day) which cover the steep part of growth curve
281 (Fig. 3A). The waste reduction (WR) and ECD were displayed in Table 1. These two
282 parameters are good indicators of feed conversion efficiency. Though no significance
283 in WR between WT and mutant, over 10% increase in ECD of *lsd1*, compared with
284 WT, suggested a better assimilation of moistened wheat bran in mutant. The lower
285 value of FCR and higher value of BE in *lsd1* also indicated mutants would show
286 better feeding performance and grow bigger or faster than WT. As mentioned above,
287 *Hilsd1* grew a little heavier (over 10%) than WT around 12th day after hatching (Fig.
288 3A), which would be contributed by the higher assimilation efficiency of *Hilsd1*.
289
290 5. The fusion lipid droplets in larvae of *HiLSD1* mutation
291 As mentioned in previous study (Kimmel & Sztalryd, 2016), LSD1 in *Drosophila*
292 *melanogaster* located on surface of lipids droplets and was involved in lipid droplets
293 (LDs) fission or fusion to regulate neutral lipids metabolism. The fat body of 5th-instar
294 larvae, WT and *lsd1*(-6, -7), were dissected from the tissues attached to the cuticle and
295 released into a mounting medium containing Hoechst for nucleus staining and Nile
296 red for neutral lipids staining. As illustrated, consistent with study in *D. melanogaster*
297 (Bi et al., 2012), *Hilsd1* mutant larval fat bodied had apparently larger lipid droplets

298 than WT (Fig. 4). Given that a complete N-terminal of LSD1 (112 amino acid) is kept
299 in *lsd1*(-6, -7) due to the target site position, which is predicted to be the N-terminal
300 of a perilipin domain by Conserved Domains Search
301 (https://www.ncbi.nlm.nih.gov/Structure/cdd/wrpsb.cgi), there were incomplete LD
302 fusion in *lsd1*(-6, -7) as illustrated.
303
304 6. The impacts of *Hillsd1* in raw fat content and fatty acids profiles
305 As LDs fusion may influence the neutral lipids degradation, the raw fat content was
306 quantified by Soxhlet extraction with non-polar solvent n-hexane. Although *lsd1*
307 mutation promoted LDs fusion, raw fat content per larvae and percentage of dry
308 materials did not show any significant difference between WT and *lsd1* in 4th-instar
309 larvae, 5th-instar larvae and prepupae stage (Fig. 5AB). However, according to the
310 content per larvae, *Hilsd1* appeared to show a tendency for more fat accumulation
311 (Fig. 5A). For fatty acid profiles (Fig. 5C), no significant change was brought by *lsd1*
312 mutation.
313
314 7. Investigation of lipogenesis relevant genes in *Hillsd1*
315 To further investigate the cause of the phenotype by impaired HiLSD1, several genes
316 in insulin signaling pathway, lipolysis pathway and fatty acid metabolism pathway
317 were selected to detect the changes in expression level in 5th-instar larvae's fat body
318 (Fig. 6). For insulin signaling pathway, the expression of all selected genes, except
319 *InR*, significantly upregulated in *Hilsd1* in comparison to WT, which partially
320 illustrate the size change around 5th-instar stage (Fig. 6A). For TAG degradation, we
321 expected that *Hilsd1* mutation would upregulate *HiLSD2* like drosophila (Bi et al.,
322 2012) and activate *HSL* and *Bmm* for more TAG triglyceride. Unexpected, all the
323 three genes had no significant change which indicate a different regulation
324 mechanism from fruit fly (Fig. 6B). For fatty acid metabolism, *FAS* for *de novo*
325 lipogenesis was regulated (Fig. 6C), while fatty acid degradation pathway were
326 downregulated by less acyl-CoA provision from upstream, which had been prevented
327 by *lsd1* mutant. In fatty acid profiles of WT and *Hilsd1*, from 5th-instar larvae to
328 prepupae stage, changes in relative percentage in lauric acid (C12) and myristic acid
329 (C14) could not show the effect of the upregulated *de novo* lipogenesis for existing

330 high content. The smaller decreased margin of palmitic and palmitoleic acid content
331 in *Hilsd1* illustrated the downregulated fatty acid degradation pathway.
332
333 **Discussion**
334 LSD1 is a member of perilipin family, which is associated with lipid accumulation
335 and energy consumption in lipid droplets (Kimmel & Sztalryd, 2016).The function of
336 LSD1 has been extensively studied in murine tissues and adult flies, but the functions
337 in insect larval growth and development have been less addressed. In larvae stage of
338 drosophila, *lsd1* brought increase in relative glyceride levels only in starved condition,
339 while no significant changes were appeared in feeding condition (Bi et al., 2012). In
340 addition, the effect of growth and development may be too little to be noticed in
341 drosophila larvae. For BSF, given the main commercialized products were from larval
342 stage, including prepupae, the mutation effect on the growth, development and
343 glyceride levels would be more worthy of attention. In this study, we first
344 characterized the ortholog of *LSD1* in *H. illucens* and uncovered a widespread
345 distribution in representative dipteran species (Fig. 1). Compared with LSD1 from *M.*
346 *sexta*, orthologs of LSD1 in dipteran species were relatively conserved. Compared
347 with phylogeny relationship of species (Zhan et al., 2019), evolution of LSD1 may
348 correlate with the speciation across dipterans.
349
350 To investigate the function of *HiLSD1*, CRIPSR/Cas9 knock-out system was
351 employed to generate mutations *in vivo*. After inbreed crossing for several
352 generations, two homozygote mutants were obtained (Fig. 2). Despite of predicted
353 premature translational termination, *Hilsd1* showed no significant defects in growth
354 and development (Fig. 3). The mutant adults behaved as the same vigor as WT, which
355 was observed by naked eyes in short distance. Instead, mutants, especially *lsd1*(-6,-7),
356 grew into heavier larvae than WT in late 5th-intar stage, beyond 10% (Fig. 3A). Even
357 after pupation with weight decreasing, *lsd1* still kept the advantage in weight, which
358 was an unexpected results due to the phenotype of lean body but with equal weight in
359 mice (Tansey et al., 2001). By feeding assays, *Hilsd1* showed significantly increased
360 assimilation than WT (Table 1), which correspond with the heavier body of mutants.
361

As the same to drosophila, *Hilsd1* also caused lipid droplets fusion (Fig. 4) which indicated inhibition for lipolysis. Although no significance increase was brought in raw fat content by *lsd1* (Fig. 5A), but the tendency suggested by the changes in content per larvae implied that the relevant genes in lipid homeostasis network had been stroke by mutations in *lsd1*. Further investigation in gene expression pattern showed that insulin signaling pathway had been upregulated in *Hilsd1* mutants, which would partially explain the bigger size and obviously heavier larval weight. Lipolysis pathway was not impaired significantly by mutations, while fatty acid metabolism was affected to weaken the downstream fatty acid degradation (Fig. 5C), which contributed to the abnormal raw fat accumulation in *Hilsd1* prepupae stage.

In summary, this study initially investigated the *in vivo* function of *LSD1* in *H. illucens* and focused on its role in larval stage. The findings not only revealed the capacity of *HiLSD1* in lipid homeostasis and insect development, but also shed a light on the lipogenesis for lauric acid through inhibition of fatty acid oxidation by *lsd1*, which would lead to the elucidation of the uncommon fatty acid profiles in BSF.

Acknowledgement

The authors would like to thank the financial support for this work by the Shanghai Pudong New Area Science and Technology Development Fund (PKJ2019-C01).

Disclosure

There are no conflicts to declare.

References

Almeida, C., Rijo, P. and Rosado, C. (2020) Bioactive compounds from Hermetia illucens larvae as natural ingredients for cosmetic application. *Biomolecules*, 10, 1–12.

Arrese, E.L. and Soulages, J.L. (2010) Insect Fat Body: Energy, Metabolism, and Regulation. *Annual Review of Entomology*, 55, 207–225.

Beller, M., Bulankina, A. V., Hsiao, H.H., Urlaub, H., Jäckle, H. and Kühnlein, R.P. (2010) PERILIPIN-dependent control of lipid droplet structure and fat storage in Drosophila. *Cell Metabolism*, 12, 521–532.

Bi, J., Xiang, Y., Chen, H., Liu, Z., Grönke, S., Kühnlein, R.P. et al. (2012) Opposite and redundant roles of the two Drosophila Perilipins in lipid mobilization. *Journal of Cell Science*, 125, 3568–3577.

Brasaemle, D.L. (2007) The perilipin family of structural lipid droplet proteins: Stabilization of lipid droplets and control of lipolysis. *Journal of Lipid Research*, 48, 2547–2559.

Broeckx, L., Frooninckx, L., Slegers, L., Berrens, S., Noyens, I., Goossens, S. et al. (2021) Growth of black soldier fly larvae reared on organic side-streams. *Sustainability (Switzerland)*, 13.

Fawole, F.J., Labh, S.N., Hossain, M.S., Overturf, K., Small, B.C., Welker, T.L. et al. (2021) Insect (black soldier fly larvae) oil as a potential substitute for fish or soy oil in the fish meal-based diet of juvenile rainbow trout (Oncorhynchus mykiss). *Animal Nutrition*, 7, 1360–1370. Chinese Association of Animal Science and Veterinary Medicine.

Gao, Z., Deng, W. and Zhu, F. (2019) Reference gene selection for quantitative gene expression analysis in black soldier fly (Hermetia illucens). *PLoS ONE*, 14, 1–14.

Generalovic, T.N., McCarthy, S.A., Warren, I.A., Wood, J.M.D., Torrance, J., Sims, Y. et al. (2021) A high-quality, chromosome-level genome assembly of the Black Soldier Fly (Hermetia illucens L.). *G3*, 11.

Hawkey, K.J., Lopez-Viso, C., Brameld, J.M., Parr, T. and Salter, A.M. (2021) Insects: A Potential Source of Protein and Other Nutrients for Feed and Food. *Annual Review of Animal Biosciences*, 9, 333–354.

Heuel, M., Sandrock, C., Leiber, F., Mathys, A., Gold, M., Zurbrügg, C. et al. (2021) Black soldier fly larvae meal and fat can completely replace soybean cake and oil in diets for laying hens. *Poultry Science*, 100.

Huis, A. Van, Oonincx, D.G.A.B., Rojo, S. and Tomberlin, J.K. (2020) Insects as feed : house fly or black soldier fly ? *Journal of Insects as Food and Feed*, 6, 221–229.

Kim, C.H., Ryu, J., Lee, J., Ko, K., Lee, J.Y., Park, K.Y. et al. (2021) Use of black soldier fly larvae for food waste treatment and energy production in asian countries: A review. *Processes*, 9, 1–17.

Kimmel, A.R. and Sztalryd, C. (2016) The Perilipins: Major Cytosolic Lipid Droplet-Associated Proteins and Their Roles in Cellular Lipid Storage, Mobilization, and Systemic Homeostasis. *Annual Review of Nutrition*, 36, 471–509.

Li, G.Y., Liu, X.J., Fang, G.Q., Yang, J., Zhan, S. and Li, M.W. (2022) Functional characterization of a low-density lipoprotein receptor in the lepidopteran model, Bombyx mori. *Insect Science*, 1–13.

Li, S., Yu, X. and Feng, Q. (2019) Fat Body Biology in the Last Decade. *Annual Review of Entomology*, 64, 315–333.

Lu, X., Gruia-Gray, J., Copeland, N.G., Gilbert, D.J., Jenkins, N.A., Londos, C. et al. (2001) The murine perilipin gene: The lipid droplet-associated perilipins derive from tissue-specific, mRNA splice variants and define a gene family of ancient origin. *Mammalian Genome*, 12, 741–749.

Nguyen, H.C., Liang, S.H., Doan, T.T., Su, C.H. and Yang, P.C. (2017) Lipase-catalyzed synthesis of biodiesel from black soldier fly (Hermetica illucens): Optimization by using response surface methodology. *Energy Conversion and Management*, 145, 335–342. Elsevier Ltd.

Niyonsaba, H.H., Hohler, J., Kooistra, J., van der Fels-Klerx, H.J. and Meuwissen, M.P.M. (2021) Profitability of insect farms. *Journal of Insects as Food and Feed*, 7, 923–934.

Raksasat, R., Lim, J.W., Kiatkittipong, W., Kiatkittipong, K., Ho, Y.C., Lam, M.K. et al. (2020) A review of organic waste enrichment for inducing palatability of black soldier fly larvae: Wastes to valuable resources. *Environmental Pollution*, 267, 115488. Elsevier Ltd.

Ribeiro, N., Costa, R. and Ameixa, O.M.C.C. (2022) The Influence of Non-Optimal Rearing Conditions and Substrates on the Performance of the Black Soldier Fly (Hermetia illucens). *Insects*, 13.

Surendra, K.C., Tomberlin, J.K., van Huis, A., Cammack, J.A., Heckmann, L.H.L. and Khanal, S.K. (2020) Rethinking organic wastes bioconversion: Evaluating the potential of the black soldier fly (Hermetia illucens (L.)) (Diptera: Stratiomyidae) (BSF). *Waste Management*, 117, 58–80. Elsevier Ltd.

Tansey, J.T., Sztalryd, C., Gruia-Gray, J., Roush, D.L., Zee, J. V., Gavrilova, O. et al. (2001) Perilipin ablation results in a lean mouse with aberrant adipocyte lipolysis, enhanced leptin production, and resistance to diet-induced obesity.

Proceedings of the National Academy of Sciences of the United States of America, 98, 6494–6499.

Walther, T.C., Chung, J. and Farese, R. V. (2017) Lipid droplet biogenesis. *Annual Review ofCell and Developmental Biology*, 33, 1–20.

Wang, C., Qian, L., Wang, W., Wang, T., Deng, Z., Yang, F. et al. (2017) Exploring the potential of lipids from black soldier fly: New paradigm for biodiesel production (I). *Renewable Energy*, 111, 749–756. Elsevier Ltd.

Xiong, J., Mao, J., Wang, T., Feng, W., Wang, W., Yang, C. et al. (2020) Refining and Sulfurization of Oil from Black Soldier Fly and Its Application as Biodegradable Lubricant Additive. *JAOCS, Journal of the American Oil Chemists' Society*, 97, 1243–1251.

Zhan, S., Fang, G., Cai, M., Kou, Z., Xu, J., Cao, Y. et al. (2019) Genomic landscape and genetic manipulation of the black soldier fly Hermetia illucens , a natural waste recycler. *Cell Research*.

Zheng, L., Li, Q., Zhang, J. and Yu, Z. (2012) Double the biodiesel yield: Rearing black soldier fly larvae, Hermetia illucens, on solid residual fraction of restaurant waste after grease extraction for biodiesel production. *Renewable Energy*, 41, 75–79. Elsevier Ltd.

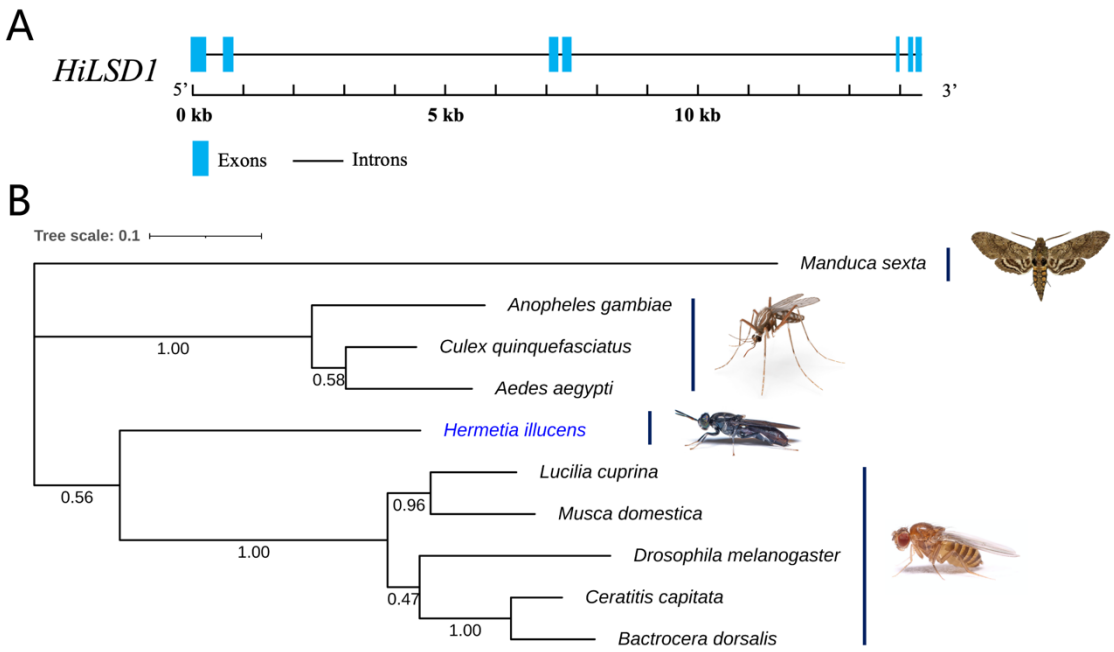

Fig.1 The genome structure of *HiLSD1* and evolutionary relationship among representative dipteran insects. (A) Schematic of *HiLSD1* gene. The blue boxes represent exons, and the solid lines represent introns. (B) Phylogenetic analysis of HiLSD1. The analysis involved 10 amino acid sequences, using LSD1 from *M. sexta* as outgroup. *Hermetia illucens* is highlighted in blue.

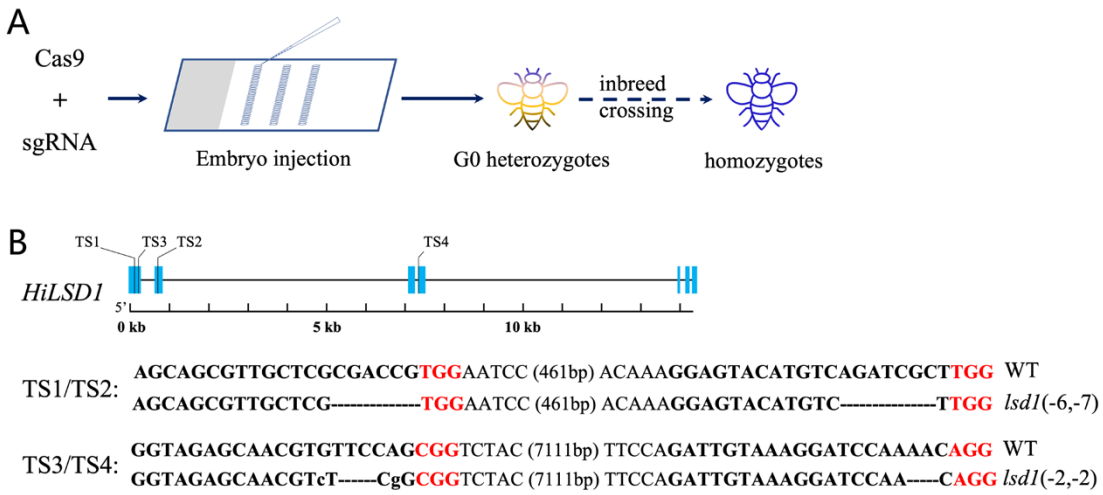

Fig. 2 CRISPR/Cas9 mediated mutagenesis of *HiLSD1* for loss-of-function homozygotes. (A) Graphic workflow of *Hilsd1* construction. Colorful fly represents heterozygotes, and blue one represents homozygotes. (B) Schematic mutagenesis target sites (TS) of *HiLSD1* and genotype of obtained homozygotes. PAM sequences are shown in red and TS sequences are in bold black. Dashed lines indicate deleted base pairs and lowercase letters mean mutated base pairs. Number of deleted base pairs is shown in the brackets.

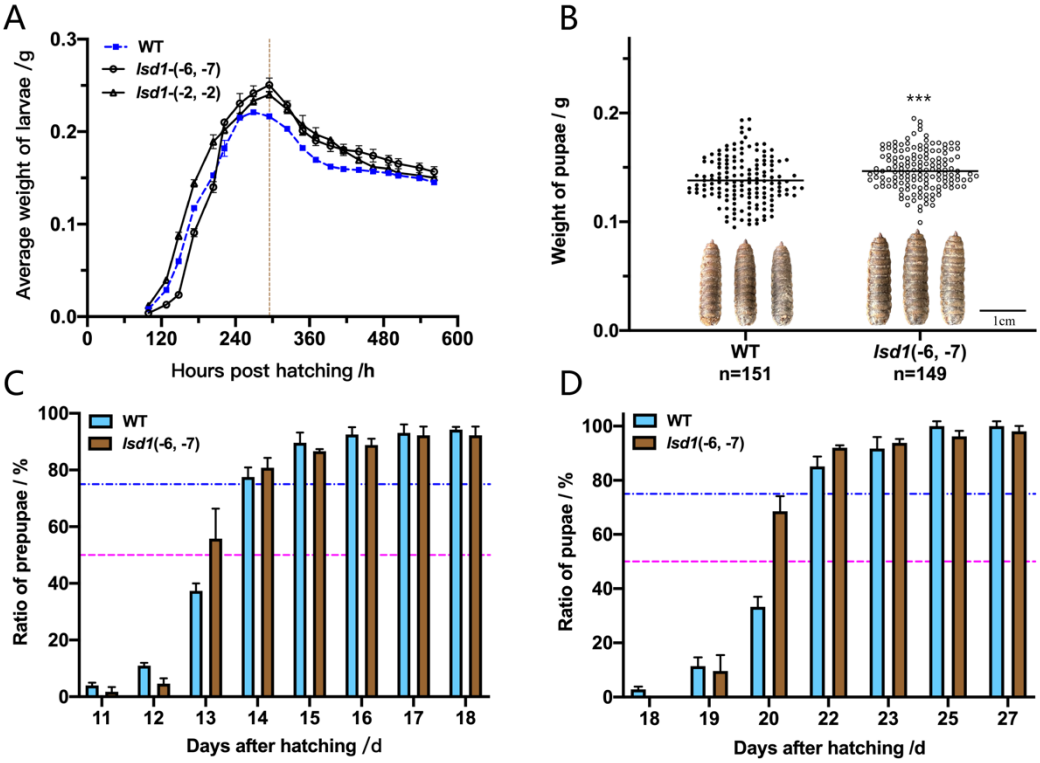

Fig. 3 Phenotype of *Hilsd1* in larval growth and development. (A) Changes in the larval weight during the growth until late pupae stage. Blue dashed line indicates wild type (WT) while hollow circle and triangle represents *lsd1*(-6, -7) and *lsd1*(-2, -2), respectively. Vertical dashed line at 295h points the maximum weight of mutants. (B) Pupae weight of WT and *lsd1*. Solid lines across the dots indicated the mean of the weight. Differences of pupae weight between WT and *Hilsd1* were tested by Welch's test. (C) Prepupation and pupation (D) rate of WT and *lsd1*. Magenta dashed line points at 50% and the blue one is at 75%.

505 Table. 1 Comparison of Bioconversion efficiency, feed conversion ratio, waste
506 reduction and ECD between *lsd1 (-6,-7)* and WT. Values are reported as mean ±
507 standard deviation (replicates indicated in the table as *n*). ***, $p < 0.001$; ns, no
508 significance according to Student's *t* test.

	n	Bioconversion Efficiency (%)	Feed Conversion Ratio (FCR)	Waste reduction (%)	Efficiency of Conversion of Digested feed (ECD)
WT	6	3.47 ± 0.10	11.08 ± 0.70	44.20 ± 0.34	7.86 ± 0.26
lsd1(-6, -7)	6	3.88 ± 0.07***	8.44 ± 0.25***	43.49 ± 1.52ns	8.92 ± 0.37***

509

510

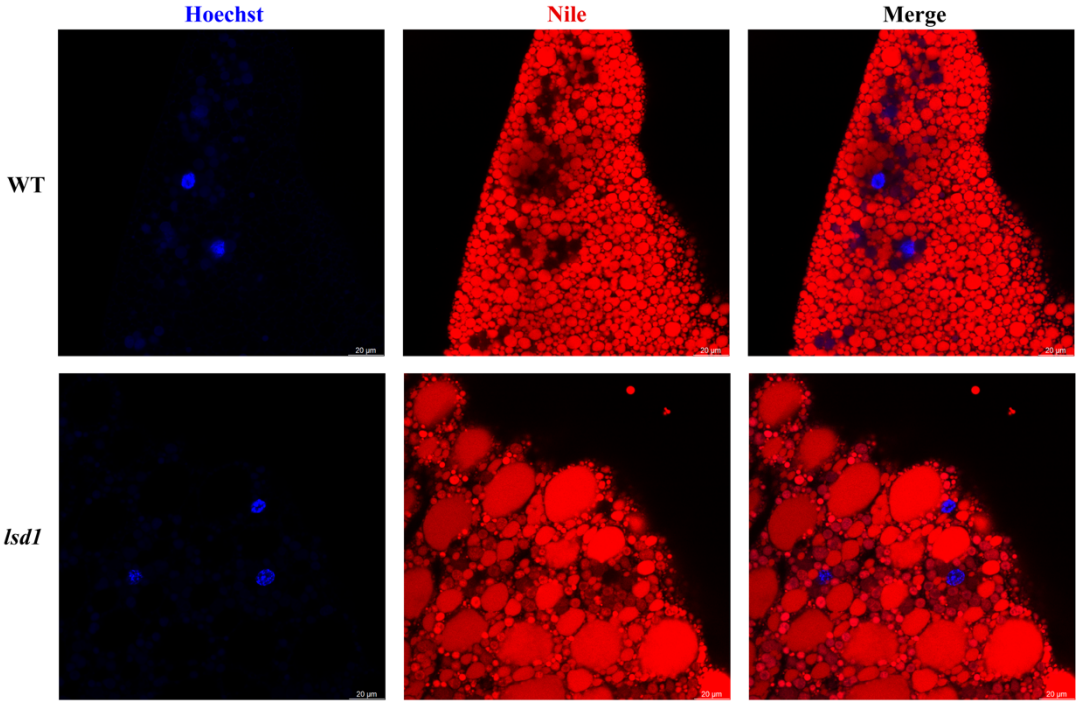

511 Fig. 4 Cellular effect of *Hilsd1* on lipid droplets in 5th-instar larvae's fat body.

512 Nucleus (blue) and neutral lipids (red) were simultaneously stained with Hoechst and

513 Nile red, respectively.

514

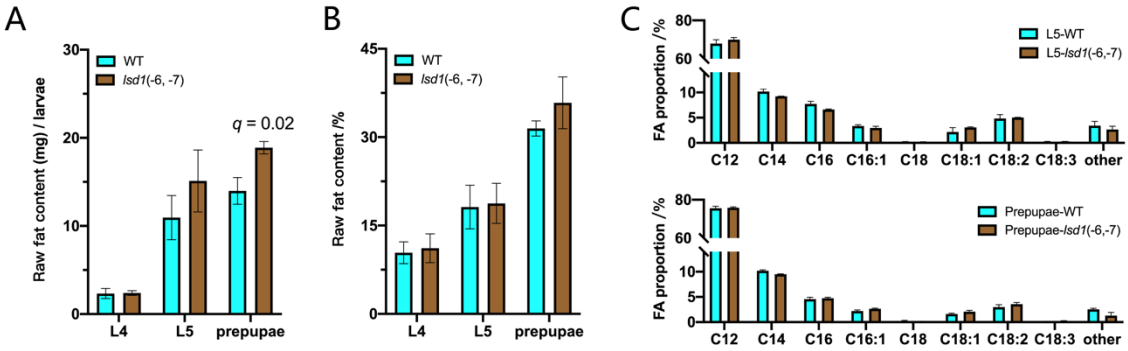

Fig. 5 The impacts of *Hilsd1* on raw fat content and fatty acid profiles. (A) Raw fat content per larvae or percentage of dray weight (B) and fatty acid (FA) profiles (C) of WT and *Hilsd1* in different stages: 4th & 5th-instar larvae and prepupae.

521

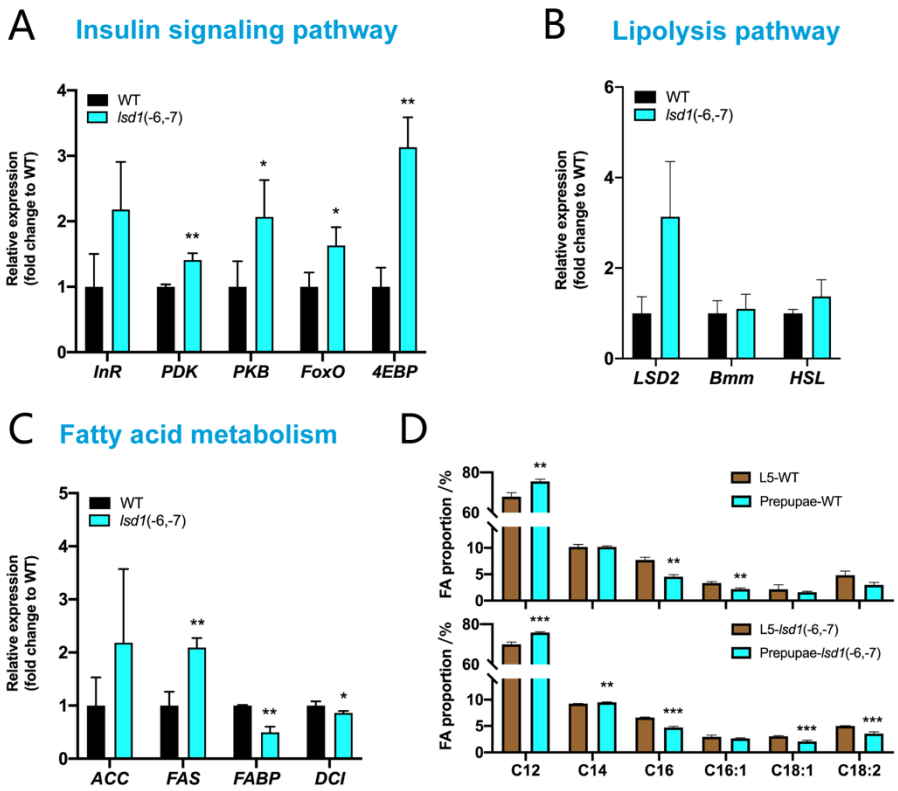

522 Fig. 6 Changes in mRNA levels of relevant pathway and fatty acid profiles in growth.
523 The relative mRNA levels of relevant genes in fat body of the 5th-instar larvae were
524 determined using *Actin* as a control. (A) *InR*, *PDK*, *PKB, FoxO* and *4EBP* were
525 chosen to detect changed in insulin signaling pathways; (B) *LSD2*, *Bmm* and *HSL*
526 were to detect the impact in lipolysis pathway; (C) *ACC, FAS*, *FABP* and *DCI* were
527 for fatty acid metabolism pathway. (D) Changes in fatty acid profiles from L5 to
528 prepupae in WT and *lsd1*. The data are shown as the mean ± S.D. (n=3). *, $p < 0.05$;
529 **, $p < 0.01$; ***, $p < 0.001$ according to Student's *t* test.
530
531